



Effect of non-spherical shape of dry powder aerosol drugs on their airway deposition distribution

T. Kolonits^a, Sz Kugler^a, A. Nagy^b, P. Füri^a, R. Ambrus^c, S. Kheirandish^d, A. Horváth^e,
 Á. Farkas^{a,*}

^a HUN-REN Centre for Energy Research, Konkoly Thege M. út, 29-33, 1121 Budapest, Hungary

^b HUN-REN Wigner Research Centre for Physics, Konkoly Thege M. út, 29-33, 1121 Budapest, Hungary

^c Institute of Pharmaceutical Technology and Regulatory Affairs, Faculty of Pharmacy, University of Szeged, Eötvös u.6, H-6720 Szeged, Hungary

^d Eötvös Loránd University, Egyetem tér 1-3, H-1053 Budapest, Hungary

^e Pulmonology Center of the Reformed Church in Hungary, Munkácsy M. u.70, 2045 Törökbálint, Hungary

ARTICLE INFO

Keywords:

Aerosol drug delivery
 Aerodynamic characterization
 Irregular particle shape
 Particle shape factors
 Airway deposition

ABSTRACT

In the majority of aerosol drug deposition modelling efforts, the particles are approximated by regular spheres. However, microscope images acquired after drug formulation available in the open literature suggest that their shape is not regular in most of the cases. This work aimed to combine experimental measurements and numerical simulations to reveal the shape factors of the particles of commercialized aerosol drugs and the effect of non-sphericity on the lung deposition distribution of these drugs. Aerosol particles of Bretaris® Genuair®, Buventol® Easyhaler® and Trelegy® Ellipta® were collected on the stages of a Next Generation Impactor after their emission from the dry powder inhalers. The samples were analyzed using scanning electron microscopy techniques. Aspect ratios and dynamic shape factors characteristic of particles in the size fractions representing each impactor stage were determined. Computer modelling of their airway deposition was performed by both neglecting and considering their irregular shape. The results of particle size measurements revealed that there was no size-specific shape factor of the particles, as they could be well characterized by a global shape factor. Although there was some inter-drug difference in terms of shape factors, the values were quite close to unity (usually between 1.02 and 1.06), except for the fiber-shaped particles representing a minority in the composition of Trelegy® Ellipta®, which could be characterized by shape factors of around 1.6. The results of computer simulations of deposition distribution indicate that neglecting the irregular shape does not lead to a major distortion of the simulation results unless fiber-shaped particles are also present after the formulation.

1. Introduction

As stated in the yearly updated Global Strategy for Asthma Management and Prevention (GINA 2024) and Global Strategy for Prevention, Diagnosis and Management of COPD (GOLD 2025) documents, aerosol drugs play a key role in the management of asthma and chronic obstructive pulmonary disease (COPD). The depositing amount of active pharmaceutical ingredient (API) and the site of deposition (e.g. upper airways, bronchial airways, acinar airways, whole lung, whole respiratory tract, etc.) are important factors of the therapeutic efficiency of the aerosol drugs. While the amount of aerosol drug deposited in the extrathoracic airways has no therapeutic effect, the desired deposition distribution within the lungs depends on the type of receptors we want

to target. For instance, M3 receptors targeted by long-acting muscarinic-antagonist (LAMA) bronchodilator drugs are the most abundant in the large bronchial airways, and their density decreases with the increase of airway generation number (Mak and Barnes, 1990). On the contrary, the surface density of β -adrenoceptors targeted by long-acting beta-agonists (LABA) and short-acting beta-agonists (SABA) increases as they penetrate deeper and deeper into the lungs along the conductive airways (Carstairs et al., 1985). Finally, the deposition distribution of the anti-inflammatory inhalation corticosteroids (ICS) should be more uniform within the whole lungs (Haughney et al., 2010). One way to quantify the dose and test the deposition distribution of the different drug particles in the human airways is to measure the deposited activity of radiolabelled drugs with a gamma camera (e.g. Newman et al., 2000; Pitcairn et al.,

* Corresponding author.

E-mail address: farkas.arpad@ek.hun-ren.hu (Á. Farkas).

<https://doi.org/10.1016/j.ijpharm.2025.125209>

Received 21 November 2024; Received in revised form 8 January 2025; Accepted 9 January 2025

Available online 11 January 2025

0378-5173/© 2025 The Author(s). Published by Elsevier B.V. This is an open access article under the CC BY-NC-ND license (<http://creativecommons.org/licenses/by-nc-nd/4.0/>).

2005; DeBacker et al., 2010, among others). However, this method has several disadvantages. One of the main drawbacks is the low resolution of the deposition map (large pixel size). In addition, the realistic activity distribution is projected into a planar image, so the resulting pixel intensity is the superposition of the activity in an unknown number of overlapping airway branches and alveoli (Lizal et al., 2018). Finally, the measurement is associated with a certain radioactive dose to the subject, can be implemented only in special laboratory environments, and is also cost-intensive. On the contrary, numerical modelling is cost-effective, reproducible, safe and efficient (Farkas et al., 2015). The two main categories of numerical lung models used for quantifying drug deposition in the airways are the so-called computational fluid and particle dynamics (CFPD) models and the whole airway analytical models, also called 1D models (Hofmann, 2011). The main advantage of the CFPD models is their high resolution, but they are restricted to small parts of the complex airway geometry. Whole lung models, like the Human Respiratory Tract Model (HRTM) of the International Commission of Radiation Protection (ICRP66, 1994), can provide useful information on the regional distribution of the deposited particles if the input data characterizing the subject's breathing mode and capacity and aerodynamic properties of particles are known. An even higher resolution can be achieved by the application of the Stochastic Lung Model (SLM), which is able to calculate airway generation number (the number of airway bifurcations from the trachea to the alveolar closing sac) specific deposition distribution of the inhaled aerosol drugs (Koblinger and Hofmann, 1990). Other examples of whole airway deposition models which can be successfully applied to model the transport and deposition of medical aerosols include the multiple path particle dosimetry model (MPPD) developed by Asgharian et al. (2001), the ExposureDoseModel of Chalvatzaki et al. (2020) or the Mimetikos Preludium model (Olsson and Kassinos, 2020).

In the open literature, both types of models were applied to compute the deposition fractions of the inhaled aerosol drugs. For instance, CFPD techniques were implemented to study the airway deposition of dry powder aerosol drugs (Augusto et al., 2016; Spasov et al., 2022; Srivastav et al., 2014; etc.), assuming spherical particle shape. A review of the CFPD efforts oriented towards the quantification of drug deposition in the airways was published by Longest et al. (2019). By the same token, analytical whole lung deposition models were applied to simulate the airway deposition of aerosol drugs by Farkas et al. (2023a), Chalvatzaki et al. (2020), Olsson and Backman (2018), among others. A review of the potential use of CFPD and analytical models to support the development and approval of generic orally inhaled drug products was published by Walenga et al. (2023). The results of modelling studies can help us understand the effect of different parameters on the lung dose of aerosol drugs, as airway deposition of the inhaled aerosol drug particles is influenced by numerous factors. The main groups of such factors are the aerodynamic properties of the inhaled particles (e.g., particle density, shape, size, and its change by hygroscopic growth, evaporation, aggregation, de-aggregation), the breathing pattern (e.g., inhalation time, breath-hold time, exhalation time, inhaled volume, peak inspiratory flow) and the airway geometry (e.g., airway length, diameter, branching angle, gravity angle, occlusion etc.) of the subjects. Moreover, there is a complex relationship even among the parameters belonging to different groups defined above. For instance, in the case of dry powder aerosol drugs, the characteristics of the particles (number of emitted particles and their size-distribution) are influenced by the breathing parameters of the patients. The characteristics of aerosol particles (especially their size) can obviously affect airway deposition by influencing the deposition mechanisms, that is, diffusion, sedimentation, and impaction. If the airway geometry also has an important effect on the deposition. If the airways are contracted (asthma or COPD), the deposition probability of the inhaled particles is usually higher than for healthy subjects.

It is worth noting that all the above-mentioned modelling works assumed spherical drug particles without accounting for the effect of

particle shape, though irregular-shaped particles behave aerodynamically differently from their spherical counterparts (Leith, 1987). In CFPD models, the non-spherical shape can be considered by the inclusion of shape factors as correction factors of the drag law of spherical particles (Chhabra et al., 1999), while in the case of analytical deposition models the spherical aerodynamic diameter must be replaced by equivalent spherical aerodynamic diameter in the deposition formulas (Baláhazy et al., 1990).

As reported in the open literature, several types of particle diameters and shape factors are used in different areas of science and technology. The type of diameter used depends mostly on the experimental method applied to measure the size of aerosol particles. The most commonly used ones are the geometric, aerodynamic, optical, and projected area equivalent diameters (Huang et al., 2021). Measurements usually determine aerosol particle size in terms of either the optical or projected area-equivalent diameters, whereas model calculations of particle impacts use geometric or aerodynamic diameters. The aerodynamic diameter of aerosol drugs can be determined by cascade impactors (e.g. Next Generation Impactor, Andersen impactor). Conversions between the four types of diameters generally assume that the particle is spherical (Hinds, 1999). However, most of the 'man-made' particles (and many of the particles of natural origin) are aspherical and have substantially different aerodynamic properties from spherical particles. Therefore, it is important to consider these topological irregularities. One way of accounting for the aspherical nature is by defining shape factors, which express the degree of deviation from an ideal (e.g. spherical) shape. Several shape factors were defined, such as aspect ratio, sphericity, circularity, elongation shape factor, compactness shape factor, waviness shape factor or Corey shape factor, among others (Exner and Hougardy, 1988; Marchildon et al., 1964; Wadell, 1933; Baba and Komar, 1981).

As computational techniques in both modelling approaches (CFD and analytical) are widely available, the main reason for not considering the irregular shape of drug particles is the lack of information on their morphology (shape factor) after the emission from the inhaler. In fact, microscope images, which are routinely used to characterize aerosol drug formulations morphologically, indicate that the shape of particles is often non-spherical (Shur et al., 2016). Based on the non-spherical shape of at least some of the formulated aerosol drug particles detected by scanning microscope images (SEM), it can be hypothesized that their shape is also non-spherical after their emission from a dry powder inhaler (DPI). It is also probable that the shape factors of the aerosolized particles emitted by the inhaler are different from the ones characterizing the particles after formulation. An important and unexplored question is to what extent the deviation from the sphericity of the emitted drug particles can influence their trajectory inside the airways and the deposited dose.

The primary objective of this work was to combine experimental and numerical methods in order to determine the size-fractionated shape factors of the particles of three commercially available aerosol drugs and to quantify the effect of non-spherical shapes on their airway deposition distribution.

2. Materials and methods

Three commercially available dry powder drugs were selected for the investigation of the effect of non-spherical shape on the airway deposition of aerosol drugs. However, the methods developed and applied in this work can be used to quantify the airway deposition of any other non-spherical dry powder aerosol drug. Bretaris® Genuair® (Berlin Chemie/Menarini) is a long-acting muscarinic agonist indicated as a maintenance bronchodilator treatment to relieve symptoms in adult patients with chronic obstructive pulmonary disease. Its pharmaceutically active ingredient is aclidinium bromide, and lactose monohydrate as a carrier. On the other hand, Buventol® Easyhaler® (Orion Pharma Limited) is a short-acting beta-agonist used for the symptomatic treatment of asthma attacks and exacerbations of asthma. It contains

salbutamol sulphate as the active ingredient and lactose monohydrate as the carrier. Trelegy® Ellipta® contains three active substances called fluticasone furoate, umeclidinium bromide and vilanterol. Fluticasone furoate is a corticosteroid, while umeclidinium bromide and vilanterol belong to the group of bronchodilators. The other ingredients are lactose monohydrate and magnesium stearate.

The effect of the non-spherical shape of the particles of the selected drugs was analyzed by collecting them with a 7-stage cascade impactor, acquiring and processing SEM images to determine their shape factors, and then comparing their modelled airway deposition distributions corresponding to spherical and non-spherical shapes.

2.1. Cascade impactor measurements

A universal shape factor could be determined by collecting the emitted particles on a single sample collector. However, our scope was to check whether the particles can be characterized by such a general factor regardless of their size or if the shape factor is size-specific. Therefore, the aerosol drug samples were collected for scanning microscope analysis after their deposition on different stages of an NGI (Next Generation Impactor). Fig. 1 shows the NGI (Copley Scientific Limited, Nottingham, UK) setup, which was employed to collect samples to assess their size-dependent shape factors. Based on the European Pharmacopoeia (Eur. Pharm., 2024), this is the standard method for determining the aerodynamic size distribution of the particles dispersed from DPIs. The DPI devices were connected to the NGI with 3D printed mouthpiece adapters via an NGI induction port representing the upper airways followed by an NGI pre-separator (Copley Scientific Limited, Nottingham, UK) to remove large particles ($> 10\text{--}15\ \mu\text{m}$). The particles collected on the impactor cups were evaluated by scanning electron microscopy, for which the original NGI cups were modified. For sampling, 0.5 mm thick silicon plates were used, which were embedded in the cups to avoid affecting the flow conditions. The size of the silicon plates (wafers) was $37 \times 37\ \text{mm}^2$ for the collection cups of stages 2–7 and $60 \times 60\ \text{mm}^2$ for the cup of stage 1 and MOC. The measurements were carried out at a flow rate of 60 L/min for 4 s with a rectangular breathing waveform provided by a vacuum pump (HCP5 High-capacity pump; Copley Scientific Ltd., Nottingham, UK) in conjunction with a critical flow controller (TPK 2000; Copley Scientific Ltd., Nottingham, UK). The sample flow rate of the NGI was checked during the

measurements with a TSI 4000 thermal mass flow meter (TSI Incorporated, Shoreview, Minnesota, USA). The cut-off sizes of the NGI are 8.06, 4.46, 2.82, 1.66, 0.94, 0.55, and $0.34\ \mu\text{m}$ for stages 1–7, respectively, for the above flow rate. The measurement setup can be seen in Fig. 1.

2.2. Scanning electron microscopy

For Scanning Electron Microscopy investigations, a Thermo Fisher™ Scios™2 DualBeam™ microscope (Thermo Fisher Scientific, Waltham, Massachusetts, USA) has been used. Due to the fact that drugs are not good conductors, a relatively low beam voltage (1.37 kV) was applied to minimize the charging effect of the particles. The samples were highly sensitive to the beam power; therefore, a relatively low illuminating current density (namely 50 pA) has been utilized. An Everhart-Thornley detector (ETD) took the secondary electron signal to achieve maximal topographical resolution.

For each drug, 9 series of measurements were performed corresponding to the different parts of the cascade impactor: the pre-separator, the seven impactor stages (collection cups) and the micro-orifice collector (MOC). The particles were collected onto silicon wafers, and samples were numbered from 0 to 8, corresponding to the parts of the cascade impactor: 0 for the pre-separator, 1–7 for the impactor stages, and 8 for the MOC. The investigated areas of the wafers were different, depending on the magnification, which varied between $200 \times$ and $20,000 \times$, depending on the sample. For each sample, 100–200 images were captured during one hour.

2.3. Determination of particle diameters, aspect ratios and shape factors

As highlighted in the Introduction section, there are several types of particle diameters and shape factors. While aspect ratio, sphericity, circularity, and elongation shape factors are determined primarily by digital image processing techniques, dynamic shape factor determination requires the simultaneous measurement of different equivalent diameters, like the mobility diameter, which can be measured with SMPS; the aerodynamic diameter, which can be measured with an aerodynamic particle spectrometer; and the mass equivalent diameter, which can be measured by a single particle aerosol mass spectrometer or a centrifugal particle mass analyser (Zeller, 1985; Kazemianesh et al., 2022; Wang et al., 2022). The shape factor used in our study has the role of linking

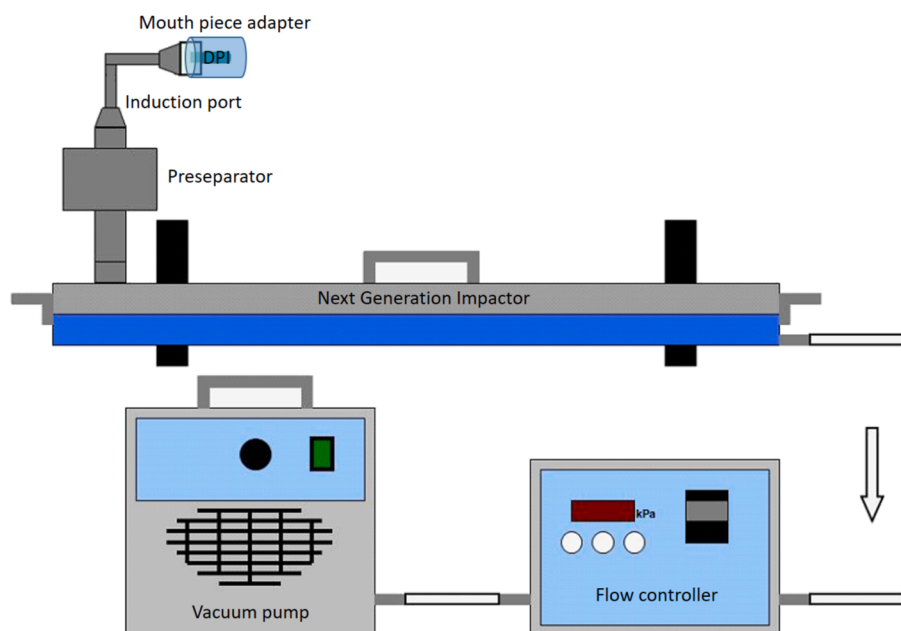


Fig. 1. The schematic design of the cascade impactor measurement setup.

the geometric diameter with the aerodynamic diameter, assuming that aerodynamic diameter is the diameter of a sphere with a unit density that has the same gravitational settling velocity as the aspherical particle with a given geometric diameter (Hinds, 1999). By the same token, the drug particles are approximated with ellipsoids, which are 3D entities.

Actually, the images acquired by the SEM method provide information on two dimensions of the particles. In this case, the particles can be modelled as ellipses, and the major and minor diameters (hereinafter a and b , respectively) can be measured (see Fig. 2. as an illustrative example).

As the particles emitted by DPIs are 3D entities, a 2D approximation may not describe the reality appropriately. Huang et al. (2021) emphasized that, especially in cases when the third dimension is significantly different from the two others, the 2D approximation leads to an incorrect equivalent diameter. Therefore, we decided to implement a 3D approximation and measure the third size, as well. The well-known “shadow effect” of the ETD detector was used to measure the height perpendicular to the Si substrate of the samples. Fig. 3 demonstrates a sample particle with shadow deposited on stage 3. It is worth noting that the figure has illustrative purpose here, and similar particles from all stages were accounted for in our analyses. As it can be seen in Fig. 3, a dark spot appears on the left side of the particles. This spot (shadow) is due to the fact that the particle absorbs a significant part of the electrons, which are backscattered from the Si substrate at the left side of the particle. It is worth noting that the backscattered electrons have a strict direction distribution and that the ETD detector is at the right side of the image (at a certain height), resulting in a shadow effect, like in the case of a spotlight illumination. Knowing the take-off angle of the ETD detector (which was calibrated by known height platinum rods and turned out to be 33.82 ± 0.27 degrees), the height perpendicular to the substrate surface of the particle can be calculated.

The samples were rotated three times by 90 degrees, and four shadows were measured for each particle to deal with the uncertainty due to the fact that the particles may not lie perfectly on the substrate. The average of these four heights (h_1 – h_4) is considered as the particle height (hereinafter referred to as c). An asymmetry factor, denoted as h^* , was also calculated from the highest and lowest height of the particle:

$$h^* = \frac{\max(\{h_1, h_2, h_3, h_4\})}{\min(\{h_1, h_2, h_3, h_4\})} - 1 \quad (1)$$

The h^* is closer to zero when the particle lays more perfectly on the substrate. In this case, the particle’s shape is closer to regular, and parameter c is closer to the particle’s real height.

Having all three dimensions (a , b , c), a volume-equivalent 3D spherical diameter (D_{eq}) can be calculated by the formula

$$D_{eq} = \sqrt[3]{abc} \quad (2)$$

It is worth noting that D_{eq} is a geometric diameter. From an aerodynamic point of view, the aerodynamic diameter is more relevant. This parameter can be obtained by using two approximations. The first approximation accounts only for the density of the particles and provides the aerodynamic diameter as

$$D_{aero} = D_{eq} \sqrt{\frac{\rho}{\rho_0}} \quad (3)$$

where ρ is the density of the particle and ρ_0 denotes the unit density.

As a second approach, the effect of non-sphericity can be accounted for by a 3D shape factor (χ). The shape-factor corrected aerodynamic diameter yielded by the formula

$$D_{aero-corr} = D_{eq} \sqrt{\frac{\rho}{\chi^3 \rho_0}} \quad (4)$$

The shape factor can be calculated with the help of

$$\chi = 0.5 * (F_s^{1/3} + \frac{1}{F_s^{1/3}}) \quad (5)$$

equation, where

$$F_s = HWR * (\frac{1}{AR})^{1.3} \quad (6)$$

In eq. (6), there are two distinct aspect ratios: the length-to-width ratio ($AR = a/b$) and the height-to-width ratio ($HWR = c/b$) (Bagheri and Bonadonna, 2016).

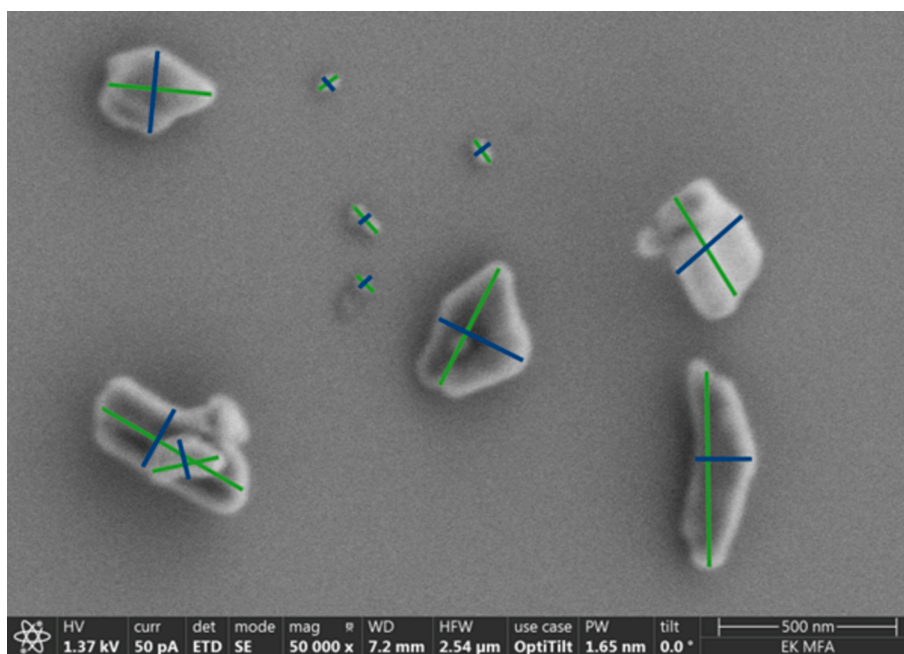


Fig. 2. SEM image of Buventol® Easyhaler® particles deposited on impactor stage 6. The major and minor diameters of the particles are highlighted with green and blue lines. Similar images are available for all the impactor stages.

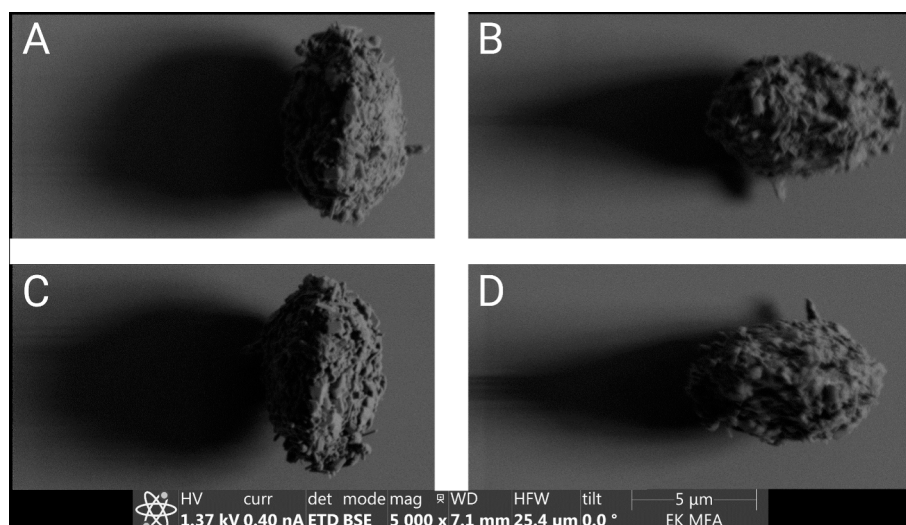


Fig. 3. SEM BSE image of a Trelegy® ELLIPTA® particle deposited on impactor stage 3. Panel A–D correspond to the original image and its rotation by 90–90 degrees.

In practice, the study of the effect of non-sphericity means the comparison between the deposition simulations assuming D_{aero} defined by eq. (3) and $D_{aero-corr}$ yielded by eq. (4).

2.4. Density measurement

In accordance with eq. (3) and (4), the determination of the aerodynamic diameter assumes the knowledge of particle density. As the density of the individual drug particles is not known (usually only the bulk and tapped densities are measured after the drug formulation, which are lower than the particle density), they were determined in this work. For this purpose, the AccuPyc II 1340 gas pycnometer (Micromeritics Instrument Corporate, Norcross, USA) was applied. This reliable, accurate technique uses the gas displacement method to measure the volume of the particle. The equipment uses helium gas as a displacement medium. In this work, a 1 cm³ sample chamber was applied for the measurements. Each aerosol drug was measured for ten cycles, and afterwards, the average density was determined. The measurements were repeated three times.

2.5. Numerical simulation of drug deposition

The most up-to-date version of the Stochastic Lung Model initially developed by Koblinger and Hofmann (1990) has been applied to quantify the amount of drug depositing in the airways assuming spherical particles (with diameters D_{aero}). For non-spherical particles, sphere-equivalent aerodynamic diameters were used ($D_{aero-corr}$). The original deposition model was presented in detail in several previous publications (e.g., Madas et al., 2020). For the sake of the reader, hereafter, we provide a brief description of the SLM.

The SLM model calculates the regional and generation number-specific deposition fractions (DF). DFs are defined here as the ratio of the particle number deposited in a certain airway region (or the whole airways) to the number of inhaled particles. In the upper airways, DF is computed with the help of empirical formulas that are valid for mouth breathing, published by Cheng (2003). The tracheobronchial airways are constructed based on the database of Raabe et al. (1980), containing morphological parameters such as tube lengths and diameters and branching and gravity angles. In this part of the respiratory tract, individual bifurcations are considered along the particle path and the corresponding deposition fractions are calculated as the contribution of inertial impaction and gravitational settling deposition mechanisms. The large number of the modelled particle pathways (10^4) ensures that

both the intrasubject and intersubject variability of the bronchial and bronchiolar structure is considered. The geometry of the acinar airways is reconstructed based on the data published by Haefeli-Bleuer and Weibel (1988). The dimension of the airways can be scaled by tuning the characteristic lung volumes, such as total lung volume and functional residual capacity (FRC), in addition to the volume inhaled by the subject (IV). In addition to these volumes, the most important inputs of the model are the particle characteristics (density and size, and shape factor corrected size in this work) and breathing data such as inhalation time (t_{in}), exhalation time (t_{ex}) and breath-holding time (t_{bh}). In this work, a reference subject with FRC = 3300 mL was considered. The breathing parameters were drug-specific as the studied drugs are dispensed in inhalers with different flow resistances. These parameters were IV = 1.81 L, t_{in} = 2.5 s, t_{bh} = 7.3 s, t_{ex} = 3 s for Bretaris® Genuair®, IV = 2 L, t_{in} = 3.4 s, t_{bh} = 7 s, t_{ex} = 3 s for Buventol® Easyhaler® and IV = 1.5 L, t_{in} = 2.1 s, t_{bh} = 7.0 s and t_{ex} = 3 s for Trelegy® Ellipta®. These series of values are averages of the breathing parameters measured by us on subjects inhaling through the three inhalers reported in Farkas et al. (2019), Farkas et al. (2023b) and Farkas et al. (2024).

Particle size and density were experimentally determined, as described above in this methods section. The numerical model briefly described above was validated for the case of medical aerosols in our earlier works (e.g. Farkas et al., 2016; Farkas et al., 2017).

3. Results and discussion

3.1. Particle densities, diameters, aspect ratios and shape factors

The results of particle density measurements revealed that the selected drugs have densities of 1570 ± 9 kg/m³, 1569 ± 6 kg/m³, and 1510 ± 6 kg/m³ corresponding to Bretaris® Genuair®, Buventol® Easyhaler® and Trelegy® Ellipta®, respectively. The close values are probably due to the fact that in all three cases, the carrier is lactose monohydrate, which is the predominant substance in terms of mass percentage. The values of the mean sphere equivalent aerodynamic diameter (D_{aero}), the mean aerodynamic diameter corrected with the dynamic shape factor ($D_{aero-corr}$), aspect ratios (AR, HWR) and shape factors (χ) of the particles deposited on the pre-separator, seven impactor stages and the micro-orifice collector determined from SEM images are presented in Table 1. The values characteristic of fibre-shaped particles found in the case of Trelegy® Ellipta® are shown separately. These fibres are deposited only on the impactor stages 4–7. Fig. 4 demonstrates a SEM image with both irregular but closer to a

Table 1

Mean aerodynamic diameter (D_{aero}) and mean shape-factor corrected aerodynamic diameter ($D_{aero-corr}$), particle aspect ratios (AR, HWR) and dynamic shape factor (χ) corresponding to the fractions of the three s deposited on different impactor stages. In the names of the samples, the first two characters refer to the drug name (BS – Bretaris® Genuair®, BU – Buventol® Easyhaler®, TR – Trelegy® Ellipta®) and the last two characters denote the parts of the impactor (00 – pre-separator, 01–07 – stages, 08 – MOC). In addition, in the case of fibre-shaped particles, the sample name includes the 'fib' suffix.

Drug name	Sample name	$D_{aero} \pm$ STD (μm)	$D_{aero-corr} \pm$ STD (μm)	AR	HWR	χ
Bretaris® Genuair®	BS00	5.068 ± 5.887	4.996 ± 5.818	1.306	0.775	1.024
	BS01	5.850 ± 3.999	5.806 ± 3.962	1.202	0.760	1.019
	BS02	5.395 ± 2.318	5.356 ± 2.302	1.215	0.831	1.014
	BS03	4.138 ± 1.430	4.110 ± 1.420	1.224	0.820	1.014
	BS04	2.204 ± 0.836	2.180 ± 0.827	1.322	0.803	1.023
	BS05	1.234 ± 0.492	1.223 ± 0.488	1.240	0.799	1.018
	BS06	1.001 ± 0.420	0.990 ± 0.416	1.244	0.803	1.020
	BS07	0.633 ± 0.242	0.625 ± 0.239	1.255	0.698	1.027
Buventol® Easyhaler®	BS08	0.910 ± 0.379	0.902 ± 0.376	1.231	0.796	1.017
	BU00	5.041 ± 6.240	4.957 ± 6.148	1.429	0.793	1.030
	BU01	9.879 ± 4.500	9.759 ± 4.447	1.275	0.765	1.024
	BU02	4.287 ± 1.948	4.194 ± 1.910	1.458	0.755	1.040
	BU03	2.234 ± 1.378	2.182 ± 1.350	1.495	0.763	1.042
	BU04	0.496 ± 0.274	0.479 ± 1.266	1.543	0.672	1.062
	BU05	0.733 ± 0.413	0.716 ± 0.405	1.477	0.737	1.042
	BU06	0.421 ± 0.180	0.414 ± 0.177	1.463	0.821	1.033
Trelegy® Ellipta®	BU07	0.346 ± 0.143	0.337 ± 0.140	1.486	0.746	1.045
	BU08	0.518 ± 0.264	0.501 ± 0.257	1.614	0.743	1.059
	TR00	7.103 ± 8.287	6.913 ± 8.119	1.356	0.671	1.042
	TR01	6.692 ± 4.501	6.562 ± 4.425	1.429	0.762	1.035
	TR02	1.674 ± 1.004	1.655 ± 0.992	1.329	0.819	1.023
	TR03	1.308 ± 0.897	1.290 ± 0.884	1.412	0.797	1.029
	TR04	0.675 ± 0.326	0.665 ± 0.321	1.401	0.779	1.030
	TR05	0.363 ± 0.170	0.357 ± 0.167	1.252	0.691	1.029
Trelegy® Ellipta® fibres	TR06	0.307 ± 0.098	0.299 ± 0.096	1.520	0.711	1.050
	TR07	0.202 ± 0.092	0.197 ± 0.089	1.592	0.753	1.052
	TR08	0.732 ± 0.209	0.723 ± 0.206	1.298	0.745	1.025
	TR04fib	0.228 ± 0.067	0.181 ± 0.053	7.725	0.560	1.630
	TR05fib	0.272 ± 0.923	0.218 ± 0.074	6.924	0.580	1.552
	TR06fib	0.202 ± 0.041	0.157 ± 0.032	8.468	0.562	1.671
	TR07fib	0.243 ± 0.135	0.194 ± 0.108	7.577	0.662	1.550

sphere and fibre-shaped Trelegy® Ellipta® particles deposited on stage 7 of the NGI impactor.

As Table 1 demonstrates, the mean diameter values decreased by stage number. This is a consequence of the decreasing collection efficiency of the stages with the decrease of particle mass as a measure of inertia. Though aspect ratios and shape factors did show some inter-drug difference, a clear tendency upon the stage number could not be demonstrated. This was also true for the fibre-shaped particles, with the remark that their shape factors were significantly higher. It is also clear from Table 1 that uncorrected and shape factor corrected values of particle diameters are not strikingly different, except for the fibre-shaped particles. This observation was true not only for the mean but also for the median values of D_{aero} and $D_{aero-corr}$. In conclusion, the results in Table 1 show that the values of the shape factors are around 1.02 and 1.04 for Bretaris® Genuair® and Buventol® Easyhaler®. The same values are 1.03 and 1.6 for the more regular and fibre-shaped particles of Trelegy® Ellipta®, respectively.

3.2. Drug deposition within the airways

Computer simulations of their airway deposition were performed following the procedure described in the Methods section to see the effect of the above-quantified irregularities of particle shape. Though Table 1 presents only the mean values of particle diameters and their STD-s, stage-specific deposition calculations were performed based on the whole size distribution in each stage. The particles were sorted in 140 size channels for the airway deposition calculations. Since airway deposition distribution of the inhaled particles is very sensitive to the diameter in the size range of 1–400 nm, a very fine (5 nm) resolution was used in this range. Between 400 nm and 2 μm , a resolution of 100 nm, in the size interval of 2–10 μm , a resolution of 500 nm, while above 10 μm , a resolution of 1 μm proved to be appropriate.

The results of drug deposition modelling in terms of regional deposition fractions (ET – that is, extrathoracic; Br – bronchial; Ac – acinar) are depicted in Fig. 5. The pre-separator (stage 0) and the first 3 stages contain high numbers of large particles. A considerable amount (about 20–35 %) of these large particles are filtered out by the upper airways (mouth, throat and larynx). The bronchial deposition is also quite high for these particles, mostly due to their impaction in the zone of airway bifurcation peaks.

A long (7 s) breath hold was simulated for all three investigated medicines, as this was the average value we measured in the clinical studies on COPD patients. Thanks to this, for stages 1–3, over 79–97 % total airway (ET + Br + Ac) deposition fraction was achieved by Bretaris® Genuair® and Buventol® Easyhaler®. For Trelegy® Ellipta® from stages 2–3, the average diameters of the measured particles were smaller than for the other two medicines, so the total airway deposition for this medicine was lower – but still quite high – in these stages. As another effect of the smaller particles, the extrathoracic deposition was also smaller in the case of Trelegy® Ellipta® for stages 2 and 3, allowing more particles to reach the lungs.

These results clearly show the importance of the long breath-hold during aerosol medicine inhalation. The inhaled particles settle with high probability by sedimentation partly in the bronchial but mainly in the acinar airways during breath-holding, which strongly decreases the exhaled amount of the drug.

As we go to stages 4–8, the particles are getting smaller and smaller. This results in smaller extrathoracic and bronchial deposition fraction values. As a consequence, more particles can reach the acinar airways. For Bretaris® Genuair®, 54–67 % of the number of inhaled particles is deposited here. For Buventol® Easyhaler® and Trelegy® Ellipta®, the acinar deposition fractions are somewhat lower but still high (over 35 %). The results also demonstrate that total deposition is lower for particles smaller than 1–2 μm . In some cases, a considerable amount of these particles is exhaled.

Comparing the regional deposition patterns corresponding to the

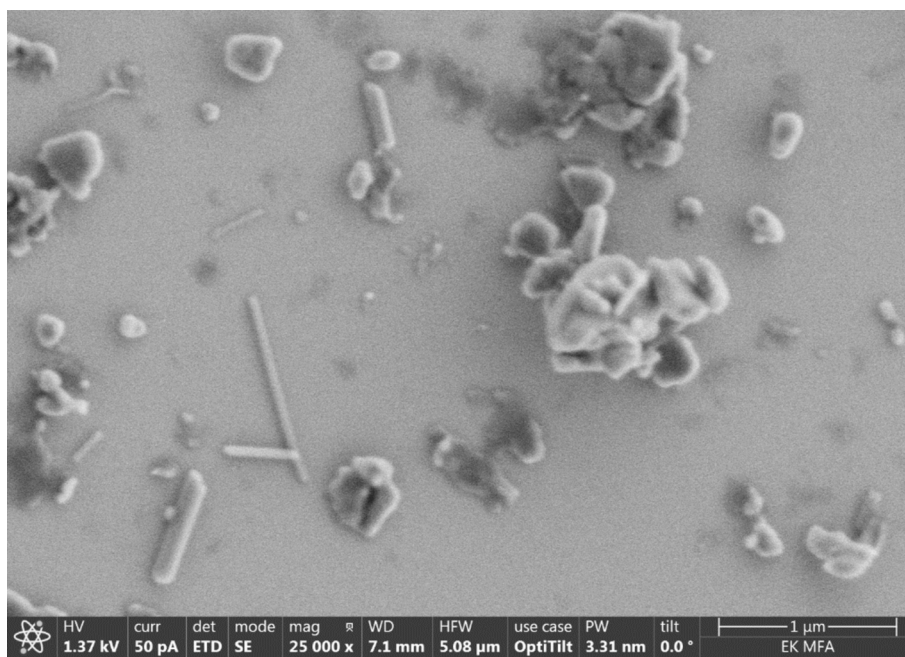


Fig. 4. SEM image of Trelegy® Ellipta® particles deposited on stage 7 of the NGI impactor. Note the fibre shape of some of the particles.

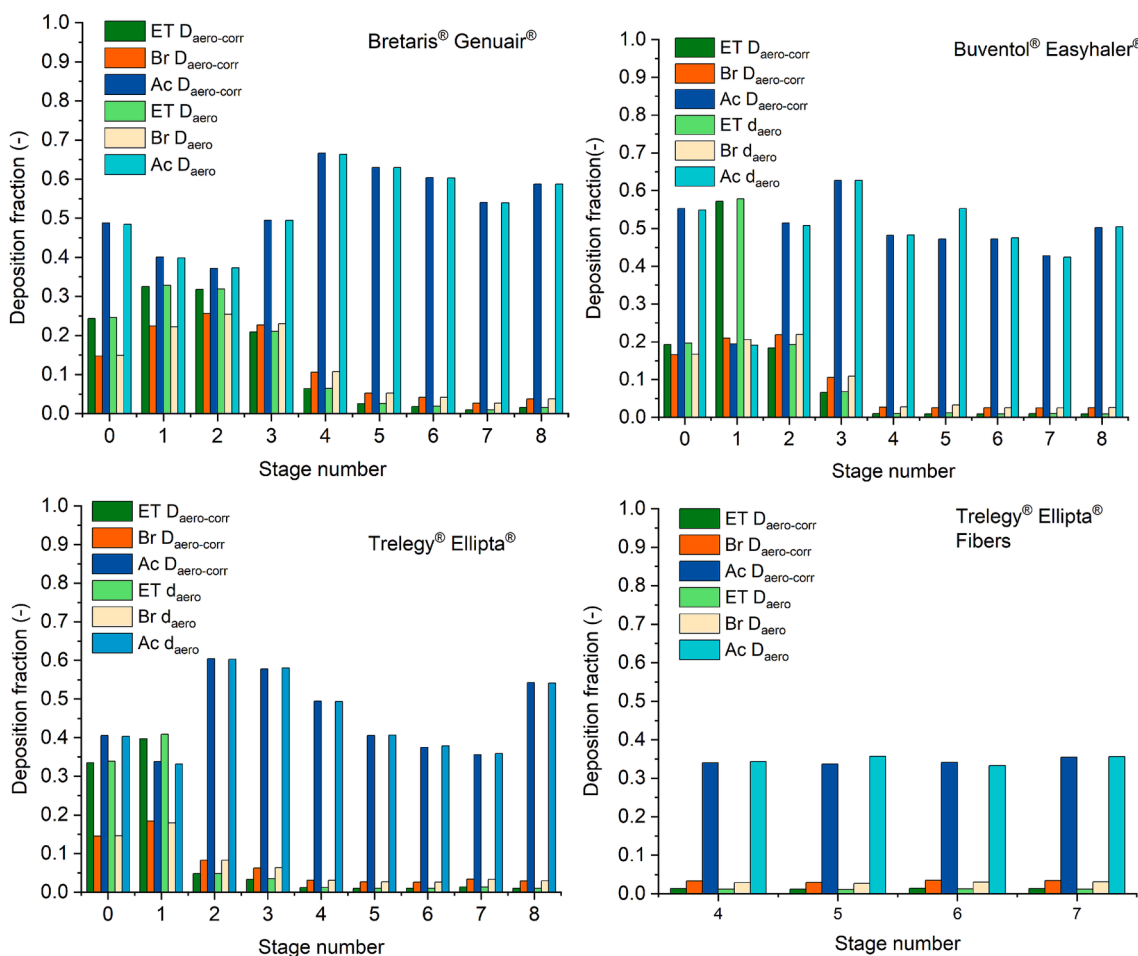


Fig. 5. Extrathoracic (ET), bronchial (Br) and acinar (Ac) deposition fractions as a function of stage number of Bretaris® Genuair® (upper left panel), Buventol® Easyhaler® (upper right panel) and Trelegy® Ellipta® (non-fibre shaped lower left panel and fibre-shaped lower right panel) aerosol drug particles.

aerodynamic diameters (D_{aero}) and dynamic shape-factor corrected aerodynamic diameters ($D_{aero-corr}$), the difference is below a few percent in all the cases. This results from the closely spherical shape (shape factor close to unity). This suggests that neglecting the differences in regional deposition fractions due to the irregular shape of the drug particles does not induce a critical error.

An exception to this behaviour is the fibre-shaped particles of Trelegy® Ellipta®. The average aspect ratios of these particles are very high (over 6.9), so there is a considerable difference between D_{aero} and $D_{aero-corr}$. For the shape-factor corrected diameters, this shifts the size distribution towards the smaller particles. It is worth noting that these fibre-shaped particles are rather small (usually between 0.15–0.3 μm), so the results cannot be compared to most of the published data involving larger (several micrometer long) fibres whose deposition was driven by inertial impaction. In the present case Brownian diffusion does play an important role in their deposition. As this thermal (Brownian) deposition increases with the decrease in particle size, the shift towards the smaller aerodynamic diameters results in higher extrathoracic and bronchial deposition fractions. Again this is in contrast with the results of studies on large fibres reporting decreased upper airway and large bronchial deposition compared to spheres (e.g. Belka et al. 2018). Although the increase of extrathoracic and bronchial deposition of Trelegy® fibers not visually seem so significant in Fig. 5 (lower left panel) in terms of relative change, they are between 10 % and 17 %. At the same time, the acinar deposition is not so sensitive to the 19–23 % change in the average diameter.

The Stochastic Lung model can provide airway generation-specific deposition distribution in a realistic, asymmetric airway structure as a special feature. Airway generation-specific deposition calculations revealed that the diameter correction with the shape factor did not cause significant differences in the deposition fraction, except for the fibre-shaped particles. Fig. 6 shows the typical bronchial deposition fraction for impactor stage 4 as a function of airway generation number. Note here that the curves obtained for stages 5 to 7 are quite similar. The figure demonstrates that bronchial deposition is lower if we neglect the irregular shape, especially around airway generations 12–18. Although in the case of Trelegy® Ellipta®, the fraction of fibre-shaped particles is low, current results suggest that it is important to consider the effect of the irregular shape if there is a considerable amount of such particles with high aspect ratios.

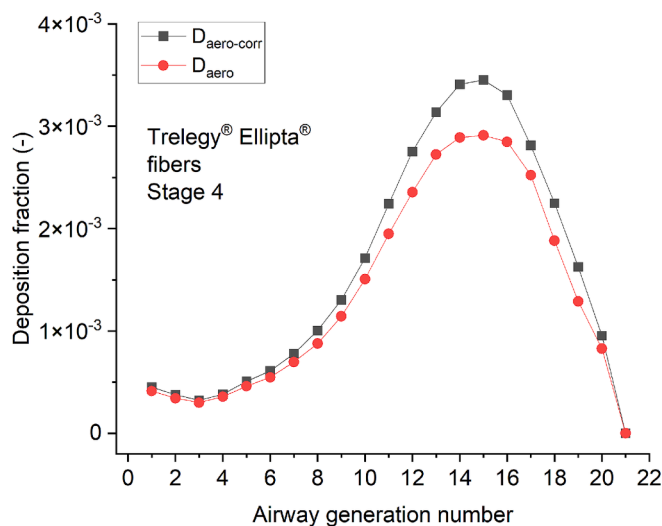


Fig. 6. Typical bronchial deposition fractions of the fibres found in Trelegy® Ellipta® with and without considering the diameter correction with the shape factor.

3.3. Limitations of the study

Obviously, besides its strengths, the method applied by us for the determination of particle diameters and shape factors has a series of limitations. Nevertheless, digital image processing techniques are now well established. They are used to determine the geometric shape factor of particles in the characterisation of cement (Mora and Kwan, 2000) in powder technology (Zheng et al., 2020), or for metal feedstock powders used in additive manufacturing (Feltner et al., 2023). Digital image processing in these applications is based on images captured with digital cameras, in our case, starting from images captured with a scanning electron microscope as described in chapter 2.2.

One of the limitations of our technique is represented by the fact that dimensions of the particles had to be measured manually, so only a limited number of particles could be considered for shape factor and airway deposition calculations. Analyzing SEM images by manually measuring the particles could also induce some errors due to human factors. However, computerized measurement by our in-house software yielded similar results, at least in terms of mean values. Another bias could be induced by the potential fragmentation of particles as a result of their impactation with the impactor plate. Theoretically, particle bounce and re-entrainment may have also occurred. In addition, superposition/coagulation of the deposited particles on the impactor plate could also occur. In addition, as it was mentioned in section 2.3., the particles may not perfectly lay on the substrate, which causes that.

(i) the height measured by the shadow length depends on the direction of the shadow (i.e. the rotation of the sample stage). We can reduce this effect by rotating and measuring the particles in different directions.

(ii) the measured height (c) is not perfectly perpendicular to the other two semi-axes of the ellipsoid (a and b), so the particle volumes are underestimated.

To characterize these effects, an asymmetry factor h^* was introduced in eq. (1). Our measurements show that the average h^* was 0.409 with a standard deviation of 0.074. There was no correlation between h^* and the kind of drug, neither the stage number nor the shape factor nor any of the particle diameters. Therefore, concerning the above-mentioned limitations, the results are consistent between the different measurements.

4. Conclusions

This study allowed us to assess the degree of irregularity of the particles of three different aerosol drugs and the effect of non-spherical shape on their airway deposition distribution. The main conclusion of the study is that most of the particles have shapes that hardly influence their fate inside the airways. An exception is the case of fiber-shaped particles, which are characterized by bigger shape factors. Therefore, all the aerosol drugs should be morphologically characterized by the methods used in this study to check the existence of highly elongated particles and their relative abundance.

CRedit authorship contribution statement

T. Kolonits: Writing – review & editing, Writing – original draft, Visualization, Methodology, Investigation, Data curation, Conceptualization. **Sz Kugler:** Writing – review & editing, Writing – original draft, Validation, Methodology, Investigation, Conceptualization. **A. Nagy:** Writing – review & editing, Validation, Methodology, Investigation, Data curation, Conceptualization. **P. Furi:** Writing – review & editing, Visualization, Methodology, Data curation, Conceptualization. **R. Ambrus:** Validation, Methodology, Formal analysis, Data curation, Conceptualization. **S. Kheirandish:** Writing – review & editing, Methodology, Formal analysis, Data curation, Conceptualization. **A. Horváth:** Writing – review & editing, Methodology, Investigation, Formal analysis, Conceptualization. **A. Farkas:** Writing – review &

editing, Writing – original draft, Supervision, Project administration, Investigation, Conceptualization.

Declaration of competing interest

The authors declare that they have no known competing financial interests or personal relationships that could have appeared to influence the work reported in this paper.

Acknowledgement

This work has been supported by the flagship project of the HUN-REN Centre for Energy Research (ID: 139). We would like to express our special thanks to Balázs Nagy (H-ION Ltd.) for the help he provided during the density measurements. The help of Dalma Günter and Veronika Oláhne Groma (HUN-REN Centre for Energy Research) in the implementation of automatized size measurements is also highly appreciated.

Data availability

Data will be made available on request.

References

- Asgharian, B., Hofmann, W., Bergman, R., 2001. Particle deposition in a Multiple-Path Model of the human lung. *Aerosol Sci. Tech.* 34, 332–339.
- Augusto, L.L.X., Lopes, G.C., Gonçalves, J.A.S., 2016. A CFD study of deposition of pharmaceutical aerosols under different respiratory conditions. *Braz. J. Chem. Eng.* 33, 549–558.
- Baba, J., Komar, P.D., 1981. Settling velocities of irregular grains at low Reynolds number. *J. Sediment. Petrol.* 51, 121–127.
- Bagheri, G., Bonadonna, C., 2016. On the drag law of freely falling non-spherical particles. *Powder Technol.* 301, 526–544.
- Balászházy, I., Martonen, T.B., Hofmann, W., 1990. Fiber deposition in airway bifurcations. *Journal Aerosol Medicine* 3, 243–260.
- Belka, M., Lizal, F., Jedelsky, J., Elcner, J., Hopke, P.K., Jicha, M., 2018. Deposition of glass fibers in physically realistic replica of the human respiratory tract. *J. Aerosol Sci* 117, 149–163.
- Carstairs, J.R., Nimmo, A.J., Barnes, P.J., 1985. Autoradiographic visualization of beta-adrenoceptor subtypes in human lung. *Am. Rev. Respir. Dis.* 132, 541–547.
- Chalvatzaki, E., Chatoutsidou, E., Lazaridis, M., 2020. Simulations of the deposition of pharmaceutical aerosols in the human respiratory tract by dry powder inhalers (DPIs). *J. Drug Delivery Sci. Technol.* 59, 101915.
- Cheng, Y.S., 2003. Aerosol deposition in the extrathoracic region. *Aerosol Sci. Tech.* 37, 659–671.
- Chhabra, R.P., Agarwal, L., Sinha, N.K., 1999. Drag on non-spherical particles: an evaluation of available methods. *Powder Technol.* 101, 288–295.
- DeBacker, W., Devolder, A., Poli, G., Acerbi, D., Monno, R., Herpich, C., Sommerer, K., Meyer, T., Mariotti, F., 2010. Lung Deposition of BDP/Formoterol HFA pMDI in Healthy Volunteers, Asthmatic, and COPD Patients. *J. Aerosol Med. Pulm. Drug Deliv.* 23, 137–148.
- European Directorate for the Quality of Medicine and Healthcare (EDQM): General Chapter 2.9.18, European Pharmacopoeia (Eur. Pharm.), 11th edition (11.3, 01/2024), 2024.
- Exner, H.E., Hougardy, H.P., 1988. Quantitative image analysis of microstructures, DGM Informationsgesellschaft mbH.
- Farkas, Á., Jókay, Á., Fűri, P., Balászházy, I., Müller, V., Odler, B., Horváth, A., 2015. Computer modelling as a tool in characterization and optimization of aerosol drug delivery. *Aerosol Air Qual. Res.* 15, 2466–2474.
- Farkas, Á., Jókay, Á., Balászházy, I., Fűri, P., Müller, V., Tomisa, G., Horváth, A., 2016. Numerical simulation of emitted particle characteristics and airway deposition distribution of Symbicort® Turbuhaler® dry powder fixed combination aerosol drug. *Eur. J. Pharm. Sci.* 93, 371–379.
- Farkas, Á., Lewis, D., Church, T., Tweedie, A., Mason, F., Haddrell, A.E., Reid, J.P., Horváth, A., Balászházy, I., 2017. Experimental and computational study of the effect of breath-actuated mechanism built in the NEXThaler® dry powder inhaler. *Int. J. Pharm.* 533, 225–235.
- Farkas, Á., Szipócs, A., Horváth, A., Horváth, I., Gálffy, G., Varga, J., Galambos, K., Sz, K., Nagy, A., Zs, S., 2019. Establishment of relationships between native and inhalation device specific spirometric parameters as a step towards patient tailored inhalation device selection. *Respir. Med.* 154, 133–140.
- Farkas, Á., Tomisa, G., Szénási, G., Fűri, P., Kugler, S., Nagy, A., Varga, J., Horváth, A., 2023a. The effect of lung emptying before the inhalation of aerosol drugs on drug deposition in the respiratory system. *Int. J. Pharm. X* 6, 100192.
- Farkas, Á., Tomisa, G., Sz, K., Nagy, A., Vaskó, A., Kis, E., Szénási, G., Gálffy, G., Horváth, A., 2023b. The effect of exhalation before the inhalation of dry powder aerosol drugs on the breathing parameters, emitted doses and aerosol size distributions. *Int. J. Pharm. X* 5, 100167.
- Farkas, Á., Horváth, A., Réti, I., Ilyés, N., Havadtó, B., Kovács, T., Sánta, B., Tomisa, G., Czaun, P., Gálffy, G., 2024. Comparative study of the inhalation parameters of COPD patients through NEXThaler® and Ellipta® dry powder inhalers. *Respir. Med.* 224, 107576.
- Feltner, L., Korte, E., Bahr, D.F., Mort, P., 2023. Particle size and shape analyses for powder bed additive manufacturing. *Particuology*.
- GINA, 2024. Global Initiative for Asthma. Global Strategy for Asthma Management and Prevention, 2024. Accessed: November 2024. Available from: www.ginasthma.org.
- GOLD, 2025. Global Initiative for Chronic Obstructive Pulmonary Disease. Global Strategy for the Diagnosis, Management, and Prevention of Chronic Obstructive Pulmonary Disease. 2025 Report. Accessed: November 2024. Available from: <https://goldcopd.org/2025-gold-report/>.
- Haefeli-Bleuer, B., Weibel, E.R., 1988. Morphometry of the human pulmonary acinus. *Anatomical Records* 220, 401–414.
- Haughney, J., Price, D., Barnes, N.C., Virchow, J.C., Roche, N., Chrystyn, H., 2010. Choosing inhaler devices for people with asthma: Current knowledge and outstanding research needs. *Respir. Med.* 104, 1237–1245.
- Hinds, W.C., 1999. Aerosol technology: Properties, behavior, and measurement of airborne particles, (2nd ed.). Wiley-Interscience.
- Hofmann, W., 2011. Modelling inhaled particle deposition in the human lung - A review. *J. Aerosol Sci* 42, 693–724.
- Huang, Y., Adebisi, A.A., Formenti, P., Kok, J.F., 2021. Linking the different diameter types of aspherical desert dust indicates that models underestimate coarse dust emission. *Geophys. Res. Lett.* 48, e2020GL092054.
- ICRP66, 1994. Human respiratory tract model for radiological protection. *Annals of the ICRP* 24, Pergamon Press.
- Kazemimanes, M., Rahman, M., Duca, D., Johnson, T.J., Addad, A., Giannopoulos, G., Focsa, C., Boies, A.M., 2022. A comparative study on effective density, shape factor, and volatile mixing of non-spherical particles using tandem aerodynamic diameter, mobility diameter, and mass measurements. *J. Aerosol Sci* 161, 105930.
- Koblinger, L., Hofmann, W., 1990. Monte Carlo modeling of aerosol deposition in human lungs. Part I: simulation of particle transport in a stochastic lung structure. *J. Aerosol Sci* 21, 661–674.
- Leith, D., 1987. Drag on non-spherical objects. *Aerosol Sci. Tech.* 6, 153–161.
- Lizal, F., Jedelsky, J., Morgan, K., Bauer, K., Llop, J., Cossio, U., Kassinos, S., Verbanck, S., Ruiz-Cabello, J., Santos, A., Koch, E., Schnabel, C., 2018. Experimental methods for flow and aerosol measurements in human airways and their replicas. *Eur. J. Pharm. Sci.* 113, 95–131.
- Longest, W., Bass, K., Dutta, R., Rani, V., Thomas, M.L., El-Achwah, A., Hindle, M., 2019. Use of computational fluid dynamics deposition modeling in respiratory drug delivery. *Expert Opinion in Drug Delivery* 16, 7–26.
- Madas, B.G., Fűri, P., Farkas, Á., et al., 2020. Deposition distribution of the new coronavirus (SARS-CoV-2) in the human airways upon exposure to cough-generated droplets and aerosol particles. *Sci Rep* 10, 22430.
- Mak, J.C., Barnes, P.J., 1990. Autoradiographic visualization of muscarinic receptor subtypes in human and guinea pig lung. *Am. Rev. Respir. Dis.* 141, 1559–1568.
- Marchildon, E.K., Clamen, A., Gauvin, W.H., 1964. Drag and oscillatory motion of freely falling cylindrical particles. *Can. J. Chem. Eng.* 42, 178–182.
- Mora, C.F., Kwan, A.K.H., 2000. Sphericity, shape factor, and convexity measurement of coarse aggregate for concrete using digital image processing. *Cem. Concr. Res.* 30, 351–358.
- Newman, S.P., Pitcairn, G.R., Hirst, P.H., Bacon, R.E., O'Keefe, E., Reiners, M., Hermann, R., 2000. Scintigraphic comparison of budesonide deposition from two dry powder inhalers. *Eur. Respir. J.* 16, 178–183.
- Olsson, B., Backman, P., 2018. Mimetikos prelude™: A new pharma-friendly aerosol drug deposition calculator. *Respiratory Drug Delivery* 1, 103–112.
- Olsson, B., Kassinos, S., 2020. On the validation of generational lung deposition computer models using planar scintigraphic images. The case of Mimetikos Prelude™. *J. Aerosol Med. Pulm. Drug Deliv.* 34, 115–123.
- Pitcairn, G., Reader, S., Pavia, D., Newman, S., 2005. Deposition of corticosteroid aerosol in the human lung by Respimat® soft mist inhaler compared to deposition by metered dose inhaler or by Turbuhaler® dry powder inhaler. *J. Aerosol Med.* 18, 264–272.
- Raabe, O.G., Yeh, H.C., Schum, G.M., Phalen, R.F., Tracheobronchial geometry: Human, dog, rat and hamster. Lovelace Foundation Report LF-53. Available at: <http://mae.engr.ucdavis.edu/wexler/lungs/LF53-Raabe/>.
- Shur, J., Price, R., Lewis, D., Young, M., Woolam, G., Singh, D., Edge, S., 2016. From single excipients to dual excipient platforms in dry powder inhaler products. *Int. J. Pharm.* 514, 374–383.
- Spasov, G.H., Rossi, R., Vanossi, A., Cottini, C., Benassi, A., 2022. A critical analysis of the CFD-DEM simulation of pharmaceutical aerosols deposition in extra-thoracic airways. *European Journal of Pharmaceutical Sciences* 629, 122331.
- Srivastav, V.K., Kumar, A., Shukla, A.K., Paul, A.R., Bhatt, A.D., Jain, A., 2014. Airflow and Aerosol-Drug Delivery in a CT Scan Based Human Respiratory Tract with Tumor Using CFD. *Journal of Applied Fluid Mechanics* 7, 345–356.
- Wadell, H., 1933. Sphericity and roundness of rock particles. *J. Geol.* 41, 310–331.
- Walenga, R.L., Butler, C., Craven, B.A., Longest, P.W., Mohamed, R., Newman, B., Olsson, B., Hochhaus, G., Li, B.V., Luke, M.C., Zhao, L., Przekwas, A., Lionberger, R., 2023. Mechanistic modeling of generic orally inhaled drug products: A workshop summary report. *CPT: Pharmacometrics and Systems Pharmacology* 12, 560–574.

Wang, S., Zhou, K., Lu, X., Chen, H., Yang, F., Li, Q., Chen, J., Prather, K.A., Yang, X., Wang, X., 2022. Online shape and density measurement of single aerosol particles. *J. Aerosol Sci* 159, 105880.

Zeller, W., 1985. Direct Measurement of Aerosol Shape Factors. *Aerosol Sci. Tech.* 4, 45–63.

Zheng, J., Sun, Q., Zheng, H., Wei, D., Li, Z., Gao, L., 2020. Three-dimensional particle shape characterizations from half particle geometries. *Powder Technol.* 367, 122–132.